Journal of the European Ceramic Society 21 (2001) 2855–2862

www.elsevier.com/locate/jeurceramsoc

Graded coatings on ceramic substrates for biomedical applications

C. Vitale Brovarone[a,*], E. Verné[a], A. Krajewski[b], A. Ravaglioli[b]

[a]*Materials Science and Chemical Engineering Department, Politecnico di Torino, C.so Duca degli Abruzzi 24, 10129 Torino, Italy*
[b]*IRTEC-CNR, Via Granarolo, 64- 48018, Faenza, Italia*

Received 15 June 2000; received in revised form 15 January 2001; accepted 20 January 2001

Abstract

Bioactive glasses and particles reinforced composites were used to coat alumina substrates, in order to combine the mechanical properties of the high-strength alumina with the bioactivity of the coatings. The coatings were either monolithic glass or glass-matrix/zirconia particle composite and were prepared by a low-cost firing method. A multilayer approach was applied to minimize crack propagation at the interface between the coating and the substrate. Functionally graded structures were developed to achieve a compliant material to withstand the stresses due to the expansion coefficient mismatch between the substrate and the coatings. The sequential coating of the alumina with glass-matrix/zirconia particle composite layers produced a structurally stable composite structure. A systematic study revealed that multiple layers were necessary to provide a gradual compliance of the thermal expansion coefficient. The glass-matrix/zirconia particles composites layers were also essential for the control of the Al^{3+} diffusion from the substrate through the glass. This is in accordance with the experimental results of previous works. Thus, the alumina content in the coating should be maintained as low as possible in order to preserve its bioactivity. The composite layers were further coated by a glass belonging to the system SiO_2–CaO–P_2O_5–Na_2O–MgO–F^-, known for its bioactivity. The experimental results were substantiated by optical and scanning electron microscopy (SEM) with compositional analysis (EDS) and by a mechanical characterization. The in vitro behavior of the coated samples was investigated by means of soaking in simulated body fluid (SBF) followed by SEM observation and XRD analysis.

Keywords: Al_2O_3-substrate; Bioactivity; Coatings; Glass matrix; Thermal expansion; ZrO_2

1. Introduction

The applications of alumina in biomedical fields are generally focused on the realization of prostheses that require good mechanical properties (i.e. load bearing bone substitutions). These devices generally show only a morphological fixation with the surrounding tissues, since they do not provide any chemical or biological bonding.[1] In addiction to alumina, several glasses have been developed for biomedical applications because of their bioactivity, i.e. the ability of forming a chemical bond to the surrounding tissues. However, because of their poor mechanical properties, the use of bioactive glasses is limited to non-load bearing applications (i.e. small bone substitutions).[2] Hence, producing glass coatings on alumina substrates may be an effective way to utilize different properties, by combining the mechanical reliability of the alumina and the bioactivity of the glass.[3]

Ceramics substrates can be easily coated by glasses by means of simple methods coming from the traditional enamels technology.[4,5] Nevertheless, there are several challenging issues remaining to be solved. For example, most of the bioactive glasses for biomedical applications, such as small bone substitution, have a thermal expansion coefficient much higher than that of alumina. For this reason a considerable residual tensile stress is induced in the glass coating, resulting in crack formation and insufficient adhesion at the interface. Alumina could be coated by glasses having a lower expansion coefficient (α) which can be obtained by a higher content of silica. An increased silica content would require a higher processing temperature and, therefore, an extensive reaction between the substrate and the glass would occur. This in turn would lead to undesirable changes in the glass composition, which would adversely affect its bioactivity.[4] Even the presence of a small amount of alumina (1.5 wt.%) in a glass can markedly affect its bioactivity resulting in a bioinert behavior.

The aim of the work is to engineer a low-cost process that would provide adherent and crack-free bioactive

---

* Corresponding author.
E-mail address: vitale@athena.polito.it (C. Vitale Brovarone).

0955-2219/01/$ - see front matter
PII: S0955-2219(01)00223-0

glass coatings, reducing to the minimum the alumina diffusion from the substrate toward the coating surface. The approach chosen in this work is based on multilayer coatings to accommodate the challenges above described. Bioactive coatings on alumina could be produced using graded structures by means of different techniques. These are:

(a) Multilayered glass coatings, obtained by covering the ceramic substrate with a first layer of high melting glass, and a second layer of a low melting and less reactive bioactive glass.
(b) Glass–matrix composite coatings, obtained by adding a second phase into the bioactive glass, aiming to accommodate the mismatch in the substrate and the coating thermal expansion coefficients, acting as well as alumina diffusion barrier.

In this work we describe some results concerning the study of different graded bioactive coatings on alumina substrates using the latter mentioned method.

2. Experimental

Full density alumina substrates were coated by different glasses belonging to the following systems: SiO_2–CaO,[6] SiO_2–CaO–B_2O_3,[7] SiO_2–CaO–Na_2O–P_2O_5,[8] SiO_2–CaO–P_2O_5–Na_2O–MgO–F^-.[4,9,10] The chemical compositions of these glasses are reported in literature (see specific references). Each glass was prepared by intimate mixing of the starting products and subsequent melting in a platinum crucible at temperatures ranging from 1450 to 1600°C. The melt was quenched in cold water in order to obtain powders, or poured on a preheated stainless steel sheet, in order to obtain bars. The bars were successively annealed, cut and polished up to a 1 μm diamond paste, up to a final size of $50\times7\times3$ mm^3. The thermal properties of each glass and their characteristic temperatures have been studied by differential thermal analysis (DTA, Netzsch mod 404S). The thermal expansion coefficients of the glasses and of the alumina substrates were measured on bars using a Netzsch dilatometer. These results are summarized in Table 1 (the different glasses have been labeled with a progressive number). The quenched glass were powdered in a ball mill and sieved below 70 μm. In order to prepare the particle reinforced composites, these powders were mixed with different percentages of yttria-stabilised zirconia particles (ZrO_2–3%Y_2O_3, Tosho, grain size <44 μm) ranging from 40 to 70%vol. The mixed powders were fired on the alumina substrates in sequenced steps to provide multilayered composite coatings. The first layer in contact with the alumina was in any case a composite one realized by using a high-melting (= low α) glass-matrix layer, aiming to achieve an appropriate match of linear expansion coefficient of the coating and the substrate. On this first layer one or more further layers were applied, using glass matrices with a progressively lower liquid temperature range (= higher α), in order to provide a good wetting between the different glasses without inducing a too high softening of the inner layers. One or two outer layers of monolithic bioactive glass (S4) were always applied on the composite ones to impart a bioactive behavior to the external surface of the coating. For comparative purposes, some specimens were prepared by adding 20% vol. of hydroxylapatite (HAp) particles to the outer layer to improve their in vitro behavior. The firing processes were optimized, step-by-step, on the basis of each glass properties. Each sample was characterized by optical and Scanning Electron Microscopy (SEM, Philips 525 M) and compositional analysis (Energy Dispersive Spectroscopy, EDS- EDAX 9100), in order to evaluate if any compositional modification occurred during the firing process.

Table 1
The different glass systems utilized and their thermal expansion coefficients

Glass	α (°C^{-1})
S1 SiO_2–CaO–Na_2O–P_2O_5–F^-	9.0×10^{-6}
S2 SiO_2–CaO	10.3×10^{-6}
S3 SiO_2–CaO–B_2O_3	10×10^{-6}
S4 SiO_2–CaO–P_2O_5–Na_2O–MgO–F^-	12.0×10^{-6}

A mechanical test, aiming to apply a shear stress at the coating/substrate interface was performed in order to verify the adhesion strength of the coating itself. The

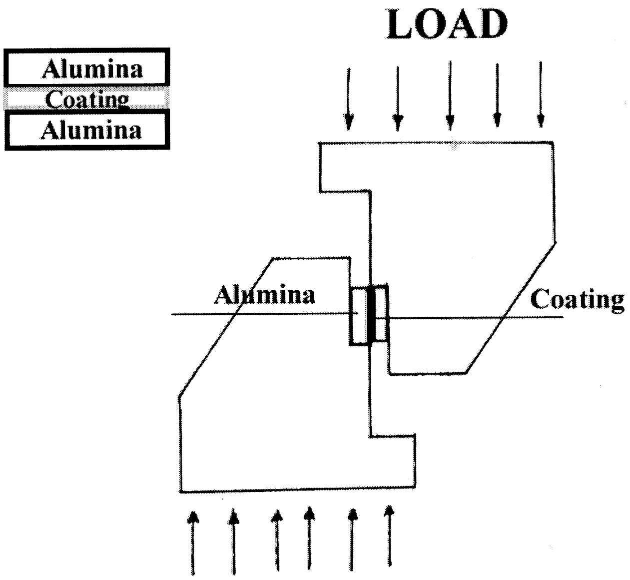

Fig. 1. Schematic representation of the adhesion test.

configuration of this mechanical test used is shown in Fig. 1 and was already used in others works.[5]

In vitro tests were carried out on the most promising samples by soaking them in SBF. After 1 and months of immersion in SBF, the samples were analyzed by means of XRD analysis and SEM observations, in order to evaluate the precipitation of a crystalline HAp layer on their surfaces.

3. Results and discussion

Table 2 shows the composition, the stacking sequences, the utilized thermal treatment and the total coating thickness of some representative samples. The composition of the composite coatings, summarized in the first two columns of Table 2, shows that a high content of reinforcing phase was utilized to prepare the composite coatings. The pertinent Y-PSZ content was identified on the basis of preliminary studies aiming to obtain crack free coatings on the alumina while maintaining a good adhesion between the coating and the substrate. These former investigations revealed that a crack free coating could be obtained reinforcing the S3 glass matrix by 60–70 vol.% of Y–PSZ. To optimize the firing process, different combinations of times and temperatures were investigated, aiming to obtain a consistent coating well adherent to the substrate. The correct firing treatment

Table 2
Processing parameters and some results on representative samples

Sample	1st Layer	2nd Layer	3rd Layer	Annealing	Thickness (μm)	wt.% Al on top
A	S1 + 70 vol.% Y-PZ 1450°C 10′	S4 + 70 vol.% Y-PZ 1350°C 10′	S4 1300°C 10′	600°C 2 h	150	9.4
B	S3 + 60 vol.% Y-PZ 1450°C 20′	S4 1300°C 15′	–	600°C 2 h	180	5.6
C	S2 + 70 vol.% Y-PZ 1450°C 20′	S4 1300°C 15′	–	600°C 2 h	150	5.2
D	S2 + 70 vol.% Y-PZ 1450°C 15′	S4 + 70 vol.% Y-PZ 1300°C 15′	S4 1300°C 10′	600°C 2 h	150	4.7
E	S2 + 70 vol.% Y-PZ 1450°C 20′	S4 1300°C 15′	S4 1300°C 10′	600°C 2 h	250	4.1
F	S3 + 70 vol.% Y-PZ 1450°C 20′	S4 1300°C 15′	S4 1300°C 10′	600°C 2 h	350	2.5
G	S3 + 70 vol.% Y-PZ 1450°C 15′	S4 + 70 vol.% Y-PZ 1300°C 15′	S4 1300°C 10′	600°C 2 h	160	2.7
H	S2 + 70 vol.% Y-PZ 1450°C 10′	S4 + 70 vol.% Y-PZ 1350°C 10′	S4 1300°C 10′ (two layers)	600°C 2 h	350	0
I	S3 + 70 vol.% Y-PZ 1450°C 10′	S4 + 70 vol.% Y-PZ 1350°C 10′	S4 1300°C 10′ (two layers)	600°C 2 h	250	0
L	S3 + 70 vol.% Y-PZ 1450°C 10′	S4 + 70 vol.% Y-PZ 1350°C 10′	S4 + 20 vol.% HAp 1300°C 10′	600°C 2 h	250	0

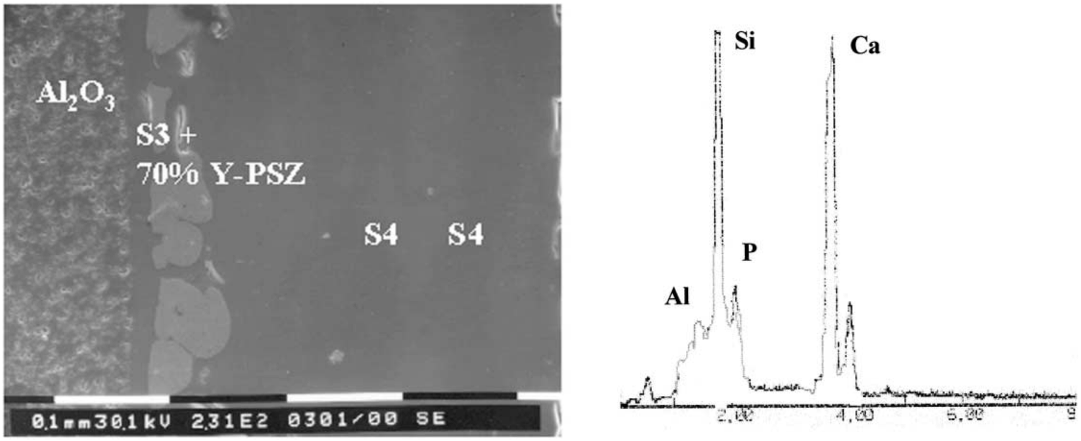

Fig. 2. Cross-section of Sample F (a) and EDS analysis performed on a 10×10 μm area situated at 20 μm from the coating surface (b).

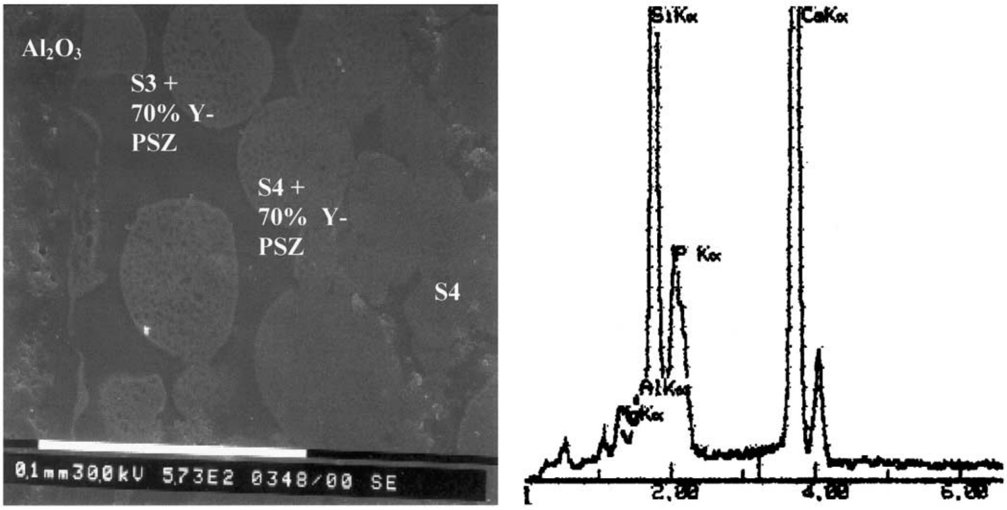

Fig. 3. Cross-section of Sample G (a) and EDS analysis performed on a 10×10 μm area situated at 20 μm from the coating surface (b).

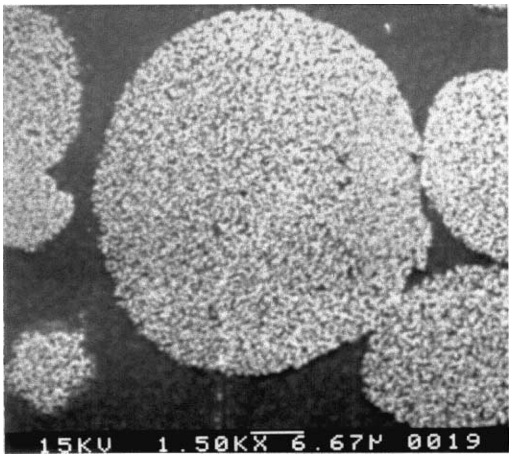

Fig. 4. SEM micrograph on an infiltrated Y–PSZ particle.

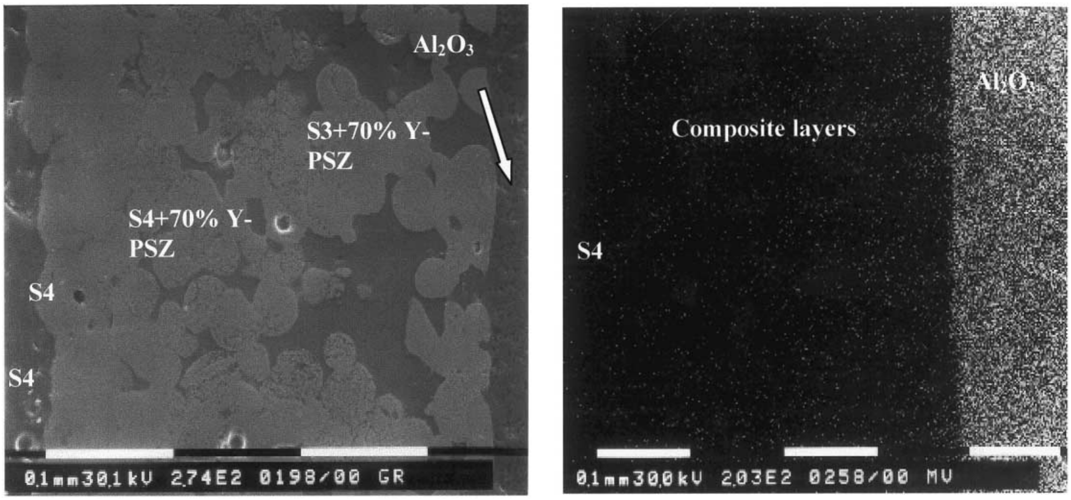

Fig. 5. Cross-section of Sample I (a) and EDS aluminium compositional map (b).

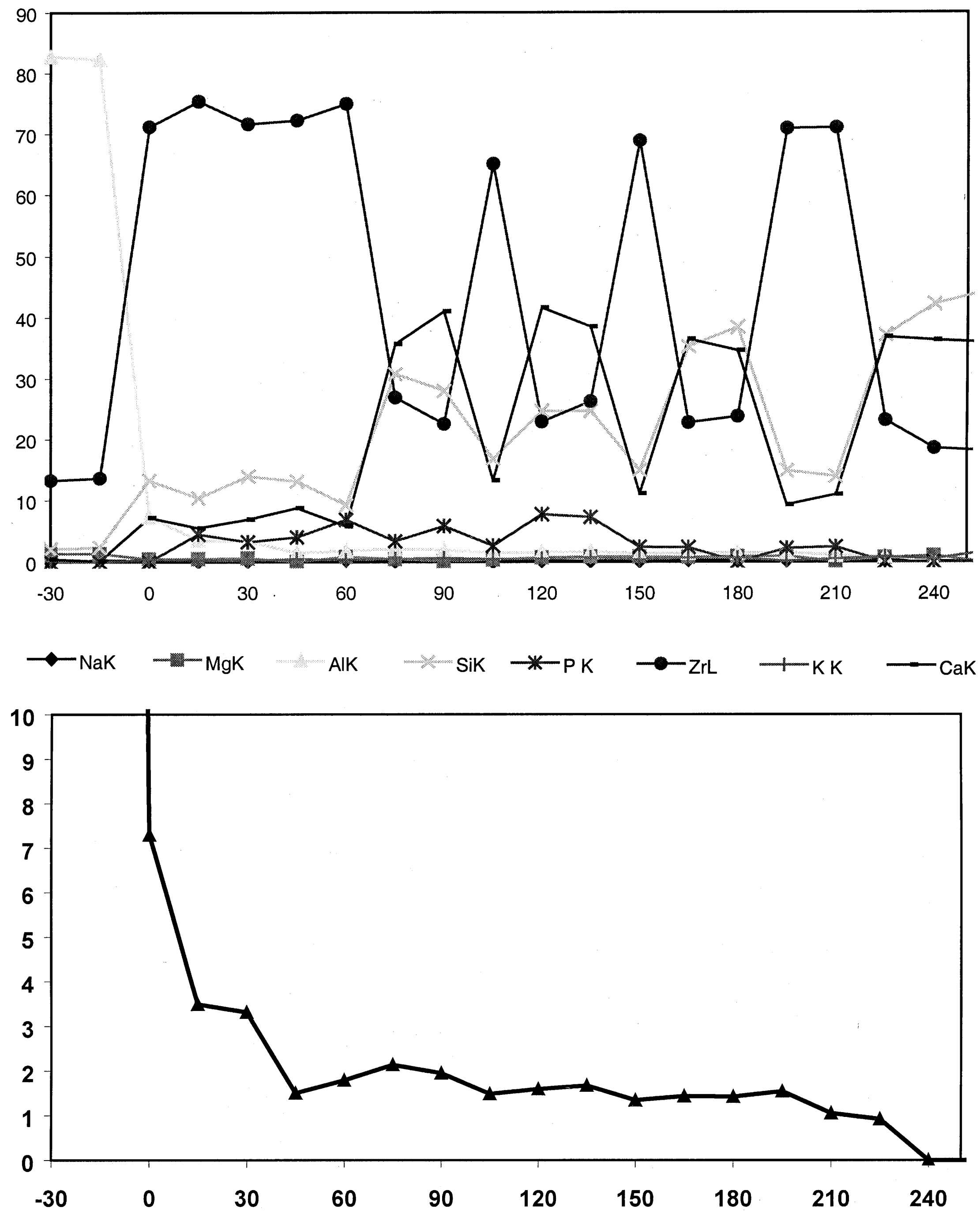

Fig. 6. (a) Elements line profile on Sample I. (b) Aluminum profile on Sample I.

was then chosen aiming to combine these latter coating characteristics with the lowest Al^{3+} diffusion in the coating itself. Using these optimized conditions crack free coatings on alumina substrates were realized. The realized coatings were well adherent to the alumina, but due to the high Y–PSZ content and the related low glass percentage, the in vitro tests did not show a bioactive behavior. Aiming to impart a bioactive behavior to the coating surface, a further monolithic S4 glass layer was applied on the composite ones. In fact, this latter glass belongs to a system known for its strong bioactivity. Due to its low viscosity at the processing temperatures, the S4 layer highly infiltrates into the zirconia particles of the underneath composite coating. For this reason, to provide a glassy outer layer and to lower the glass infiltration, a second S4 monolithic layer was applied utilizing a shorter processing time. Thus, a 20 μm glass outer layer, that should be involved in the bioactivity mechanism, was obtained. The good microstructural properties of the coatings were maintained also after the addition of these two latter S4 layers and no cracks were detected by SEM observations on the cross sections. The last column of Table 2 shows the wt.% of aluminum found by means of EDS analysis in a 10×10 μm area situated at approximately 20 μm from the coating surface. The glass S1, did not allow a satisfactory control on the Al^{3+} diffusion. Better results on the control of Al^{3+} diffusion through the coating were obtained by using the glass S2 or S3 as matrices for the first composite layer. Yet, we observed that the type of matrix is not the only one parameter that greatly affects the Al^{3+} diffusion from the substrate toward the coating. In fact, both the time and temperature of the thermal treatment revealed to have an extensive influence on the final content of alumina in the coating. Thus, the time and temperature of the thermal treatment where reduced as much as possible. Table 2 reports the time and temperature combinations of the most promising samples. The thickness of the coatings is the other main factor which influences the aluminum amount at the coating surface. In fact all the thicker samples revealed a lower aluminum when compared to the correspondent thinner samples. Aiming to lower the total thickness of the coating, without any increase in the alumina content at the surface (Sample I), the thermal treatment was further on optimized. Fig. 2a and b shows a cross-section of Sample F and the EDS analysis performed on an area at 20 μm from its surface, respectively. In Fig. 2a, a very good adhesion of the coating to the substrate and an indistinguishable interface between the three different layers, i.e. the composite (S3 matrix) and the two glassy ones (S4), is observed. Furthermore, the zirconia particles are well embedded into the glass matrix and neither porosity nor cracks are present into the whole coating. Sample F was about 350 μm thick and the EDS analysis, detected a 2.5 wt.% of aluminum on the coating surface. This latter value is lower than those observed on other samples (see for example Samples A–E, Table 2) but it is still not low enough to avoid the inhibition of the bioactivity mechanism due to the reduction of the glass solubility and the ionic exchange in SBF. Better results were obtained with Sample G that was realized by preparing two composite layers (with two different glass matrices, i.e. S3 and S4) and only one glassy layer (S4) on top of them. A comparison between the EDS results obtained on Samples F and G shows that the aluminum contents at the coatings surface are similar. Yet, in the case of Sample G, an optimization of the coating preparation, allowed to obtain a coating only 160 μm thick. Fig. 3a and b depict the cross-section

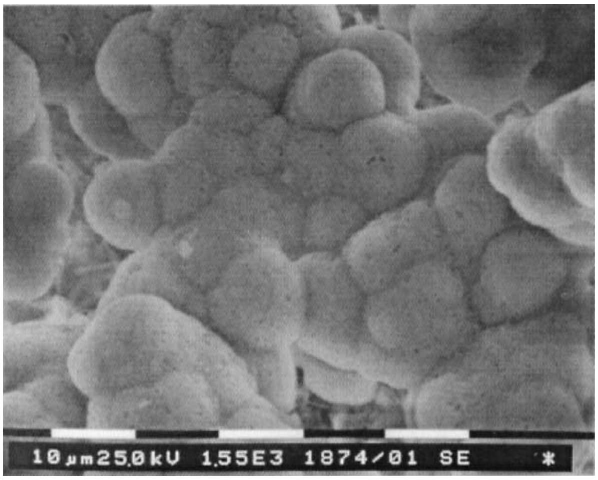

Fig. 7. Sample L: SEM after 2 months in SBF.

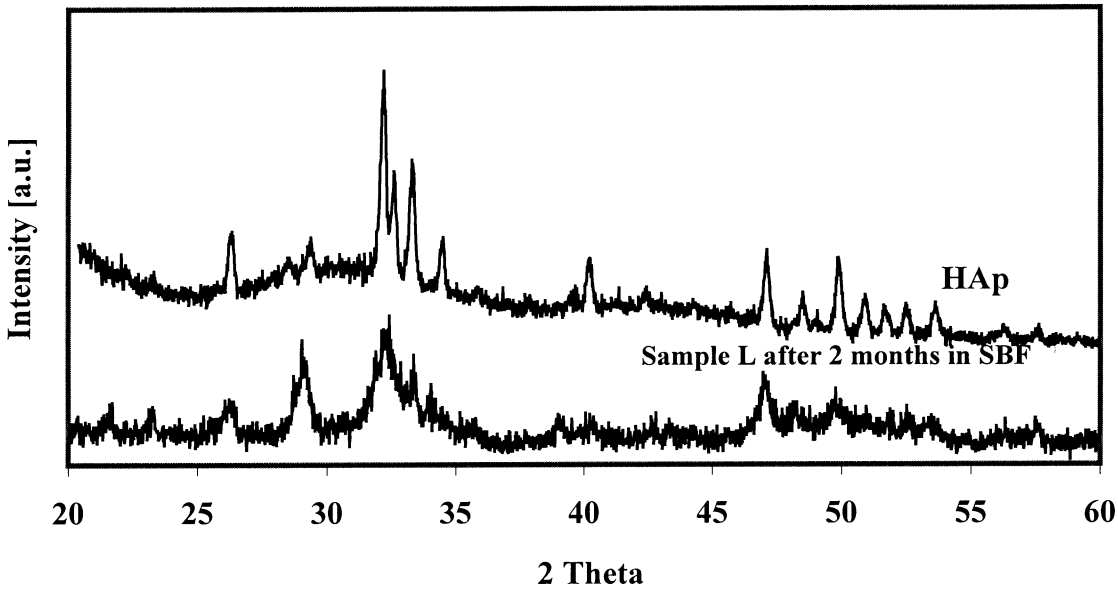

Fig. 8. XRD results on sample L after immersion in SBF for 2 months.

of Sample G and the EDS analysis performed on the coating surface, respectively. The SEM observation on the cross section shows a very good adhesion of the coating to the substrate and a very good quality of the coating itself, as no porosity or cracks were found. Fig. 4 shows that the reinforcing phase is very well embedded into the glass matrix and that the glass matrix infiltrates into the zirconia particles. These considerations suggest a high homogeneity of the composite layers. Aiming to lower as much as possible the Al^{3+} diffusion through the coating, a further optimization of the process was developed, leading to the production of Samples H and I, in which the coating surfaces were aluminum free. Fig. 5a, shows a cross section of Sample I, the good homogeneity and the pertinent morphological characteristics were obtained again on this 350 μm thick coating. Furthermore, the EDS map of aluminum concentration is reported in Fig. 5b and shows the lack of aluminum at the coating surface. Fig. 6a and b depicts the elements and the aluminum line profiles obtained on Sample I acquiring 20 spots along the whole coating section. The data reported in Fig. 6a show that the glass matrix infiltrates the reinforcing particle. Fig. 6b demonstrates that the aluminum content is lowered both from the coating thickness and from the presence of the dispersed phase. As described elsewhere,[11] an extensive biological evaluation, using fresh rat osteoblasts, has been performed on a set of specimens prepared in the same condition of sample I, and a very good degree of biocompatibility was determined. Though no aluminum was detected at the outer coating surface of sample I, the coating did not show a strong in vitro bioactive behavior, in terms of HAp precipitation during soaking in SBF. The reaction layer produced on their surface after 1 month of soaking in SBF was too weak to be clearly detected by SEM or XRD. For this reason, sample L was prepared adding in the outer layer 20 vol.% of HAp particles. The addition of HAp particles didn't involve any detrimental effect on the coating quality and any cracks or porosity was observed on these samples. This approach allowed to obtain a substantial HAp precipitation on the coating surface after immersion in SBF, with the typical globular morphology, as shown in Fig. 7. The XRD analysis revealed that no crystalline phases but hydroxylapatite are present on the coating surface after 2 months in SBF. For this purpose in Fig. 8 are compared the XRD spectra of pure HAp and of Sample L after soaking in SBF. The broadening of HAp signals in the pattern of Sample L is ascribable to the morphology of crystals precipitated by aqueous solutions, and is a common feature in self-grown HAp layers.

From a mechanical point of view, the adhesion test caused the failure of the glue between the substrate and the metallic grasps, without breaking the coating/substrate interface. The glue failure was caused by loads close to 25 MPa which means that the interface strength is at least of this magnitude.

4. Conclusions

Multilayered glass-matrix/zirconia particle coatings on alumina substrates were successfully obtained. The coatings were well adherent to the alumina and without residual porosity. The utilized enameling technique was engineered and optimized in order to obtain coating of pertinent thickness. The two intermediate layers of glass-matrix/zirconia particles composite satisfied the desired twofold function: they provide a gradual variation of the thermal-mechanical properties from the alumina substrate to the glassy surface and they act as a barrier to Al^{3+} diffusion. In fact, the thermal expansion coefficient of zirconia ($11.9–12.0\times10^{-6}$ /°C) is similar to the outer glassy layer one (12.0×10^{-6}/°C) and the thermal expansion of the glass-matrix of the first composite layer is close to that of alumina ($8.7–9.6\times10^{-6}$/°C). Thus, crack free coatings on alumina were obtained. The optimization of the layers compositions and stacking sequence, the firing process conditions and the total thickness allowed to control the Al^{3+} diffusion. Thus, an aluminum free outer layer was obtained. A strong bioactive behavior was observed after the addition of HAp particles to the outer glass layer. The coating adhesion strength was superior to 25 MPa.

Acknowledgements

This work was partially funded by the MURST-CNR project 1998/2000 (00002.PF32).

References

1. Hulbert, S. F., The use of alumina and zirconia in surgical implants. In *An Introduction to Bioceramics*, Vol. 1, ed. L. L. Hench and J. Wilson. World Scientific, 1993, p. 25.
2. Hench, L. L. and Bioceramics. *J. Am. Ceram. Soc.* 1998, **81**(7), 1705.
3. Ravaglioli, A., Krajewski, A., Piancastelli, A., Berger, G., Adam, K. and Gildenhaar, R., The influence of alumina porosity in glass ceramic adhesion. *Interceram.*, 1992, **41**(2), 69.
4. Ferraris, M., Verné, E., Moisescu, C., Ravaglioli, A. and Krajewski, A., Bioactive coatings on Al_2O_3 and ZrO_2. In *Bioceramic Coatings for Guided Bone Growth*, ed. A. Ravaglioli and A. Krajewski. Gruppo Editoriale Feanza Editrice, 1996, p. 31.
5. Ferraris, M., Verné, E., Appendino, P., Moisescu, C., Krajewski, A., Ravaglioli, A. and Piancastelli, A., Coatings on zirconia for medical applications. *Biomaterials*, 2000, **21**, 765–773.
6. Shelby, J. E., Effect of morphology on the properties of alkaline earth silicate glasses. *J. Appl. Phys.*, 1979, **50**(12), 8010.
7. Ferraris, M., Rabajoli, P., Brossa, F. and Paracchini, L., Vacuum plasma spray deposition of titanium particle/glass-ceramic matrix biocomposites. *J. Am. Ceram. Soc.*, 1996, **79**(6), 1515.
8. Ducheyne, P., Marcolongo, M. and Schepers, E., Bioceramic composites. In *An Introduction to Bioceramics*, ed. L.L. Hench and J. Wilson. World Scientific, 1993, p. 281.
9. Berger, G. and Gildenhaar, R., Long-term stable bioactive glass ceramic as implant material—ten years of clynical experience. *Fourth World Biomaterials Congress* 24–28 April 1992, Federal Republic of Germany, Berlin, p.33.

10. Verné, E., Ferraris, M., Ventrella, A., Paracchini, L., Krajewski, A. and Ravaglioli, A., Sintering and plasma spray deposition of bioactive glass-matrix composites for medical applications. *J. Eur. Ceram. Soc.*, 1998, **18**, 363.
11. Torricelli, P., Verné, E., Vitale Brovarone, C., Appendino, P., Krajewski, A., Ravaglioli, A., Pierini, G. and Giardino, R., Biological glass coating on ceramic materials: in vitro evaluation